Nanoscale Res Lett (2009) 4:732–737
DOI 10.1007/s11671-009-9312-z

NANO EXPRESS

New Method to Prepare Mitomycin C Loaded PLA-Nanoparticles with High Drug Entrapment Efficiency

Zhenqing Hou · Heng Wei · Qian Wang · Qian Sun · Chunxiao Zhou · Chuanming Zhan · Xiaolong Tang · Qiqing Zhang

Received: 10 February 2009 / Accepted: 2 April 2009 / Published online: 21 April 2009

Abstract The classical utilized double emulsion solvent diffusion technique for encapsulating water soluble Mitomycin C (MMC) in PLA nanoparticles suffers from low encapsulation efficiency because of the drug rapid partitioning to the external aqueous phase. In this paper, MMC loaded PLA nanoparticles were prepared by a new single emulsion solvent evaporation method, in which soybean phosphatidylcholine (SPC) was employed to improve the liposolubility of MMC by formation of MMC–SPC complex. Four main influential factors based on the results of a single-factor test, namely, PLA molecular weight, ratio of PLA to SPC (wt/wt) and MMC to SPC (wt/wt), volume ratio of oil phase to water phase, were evaluated using an orthogonal design with respect to drug entrapment efficiency. The drug release study was performed in pH 7.2 PBS at 37 °C with drug analysis using UV/vis spectrometer at 365 nm. MMC–PLA particles prepared by classical method were used as comparison. The formulated MMC–SPC–PLA nanoparticles under optimized condition are found to be relatively uniform in size (594 nm) with up to 94.8% of drug entrapment efficiency compared to 6.44 μm of PLA–MMC microparticles with 34.5% of drug entrapment efficiency. The release of MMC shows biphasic with an initial burst effect, followed by a cumulated drug release over 30 days is 50.17% for PLA–MMC–SPC nanoparticles, and 74.1% for PLA–MMC particles. The IR analysis of MMC–SPC complex shows that their high liposolubility may be attributed to some weak physical interaction between MMC and SPC during the formation of the complex. It is concluded that the new method is advantageous in terms of smaller size, lower size distribution, higher encapsulation yield, and longer sustained drug release in comparison to classical method.

Keywords Mitomycin C · PLA · Nanoparticles · Drug release

Z. Hou · H. Wei · Q. Wang · Q. Sun · C. Zhou · C. Zhan · X. Tang · Q. Zhang (✉)
Research Center of Biomedical Engineering of Xiamen University, Material College of Xiamen University, Xiamen 361005, China
e-mail: zhangqiq@xmu.edu.cn

Z. Hou
e-mail: houzhenqing@xmu.edu.cn

Q. Zhang
Chinese Academy of Medical Sciences, Peking Union Medical College Institute of Biomedical Engineering, Tianjin 300192, China

Introduction

Mitomycin C (MMC) is a bifunctional alkylating agent which has been extensively used as an anti-tumor agent for a long time. Because of MMC's enhanced activity in hypoxic environments [1], it has great potential for loco-regional treatment of solid tumors since a significant percentage of viable cancer cells within a solid tumor can be hypoxic [2]. However, use of MMC is associated with a number of acute and chronic toxicities, such as irreversible myelosuppression and hemolyticuremic syndrome, which limit its clinical application. Therefore, efforts have been made to lessen the toxic effects of MMC and improve its utility using various delivery methods.

The predominant method for MMC delivery involves drug encapsulation in nano-or micro-particles using various polymers including albumin [3], dextran [4, 5], estradiol [6], *N*-succinyl-chitosan [7], hydrogels [8], polybutylcyanoacrylate [9], and poly-epsilon-caprolactone [10]. These

systems, however, have shown some defects for local administration of MMC due to fast degradation of those drug carriers in the body.

PLA is a well-known biodegradable and biocompatible polymer and has a relatively longer degradation time in vivo (from weeks to months) according to their molecular weight. It has been used in various applications such as wound dressing and drug delivery [10, 11]. Generally, the water-limited soluble MMC cannot be directly dissolved in hydrophobic organic solvents such as dichloromethane, so the drug entrapment efficiency of PLA nano/microparticles prepared by a classical double emulsion solvent evaporation method is very limited.

In order to overcome these shortcomings, we have developed a new method to prepare mitomycin C loaded PLA nanoparticles by a new emulsion solvent evaporation technique, in which soybean phosphatidylcholine (SPC) was employed to improve the liposolubility of MMC by formation of MMC–SPC complex. SPC was used because of its good biocompatibility and ready availability.

In this paper, the four main influential factors at three levels, PLA MW (molecular weight), ratio of PLA to SPC (wt/wt) and ratio of MMC to SPC (wt/wt), volume ratio of oil phase to water phase chosen for the present investigation, were based on the results of preliminary experiments using a single-factor test; the emphasis of this paper was placed on the optimum production conditions and characterization of PLA–MMC–SPC nanoparticles in vitro.

Experimental Details

Materials

Mitomycin C (MMC) (99.5%) was purchased from Shanghai Xin Ya Pharmaceutical Co. Ltd. PLA (M_w = 5000, 10000, 50000) were obtained from Shandong Medical Treatment and Instrument Institute. Soybean phosphatidylcholine was provided by Sigma Co. Ltd. Dichloromethane (DCM), dimethyl sulfoxide (DMSO), poly (vinyl alcohol) (PVA, degree of polymerization 1700, degree of hydrolysis 88.5%) used as a stabilizer in the external water phase were purchased from Xiamen Chemical Reagents Company (Xiamen, China). All other reagents and solvents were of analytical grade.

Preparation of MMC–SPC Complex

Due to both MMC and SPC being dispersed as the unimolecular form in DMSO solution, a waterless complex of MMC and SPC was formed after removal of the solvent. So the complex was prepared by an anhydrous co-solvent lyophilization method. Briefly, MMC powder and SPC with a ratio of 1:5 (wt/wt) were co-dissolved in dimethyl sulfoxide (DMSO) by gentle agitation. The resultant homogeneous solution was then freeze-dried overnight at a condenser temperature of −40 °C and under a vacuum of 10 Pa. So the MMC–SPC complex with a ratio of 1:5 was obtained; the MMC–SPC complex with a ratio of 1:10 and 3:10 (wt/wt) were also prepared in a same way used as the following optimal experiment.

The MMC–SPC physical mixture was prepared by mixing MMC with SPC (a ratio of 1:5 wt/wt).

FTIR Analysis of Complex

Fourier transform infrared spectrophotometry (FTIR Spectrometer, BRUKER IFS-55, Switzerland) was used to study the interaction between MMC and SPC. The FTIR spectra of MMC, SPC, the complex and physical mixture of MMC and SPC with a ratio of 1:5 (wt/wt) were obtained by the KBr method.

Solubilization Studies of Complex

Organic solvent dichloromethane (DCM) was used to evaluate the altered solubility of MMC after it was combined with SPC. Briefly, aliquots of organic solvent (2 mL) were introduced into MMC–SPC complexes (20 mg) and physical mixture (20 mg) of SPC and MMC with a ratio of 5:1, respectively, followed by gentle vortexing until an equilibrium system was obtained. The solubilization of each system before and after 24 h of storage was evaluated by visual examination.

Preparation of MMC–PLA–SPC Nanoparticles

MMC was formulated into PLA nanoparticles by a new single emulsion solvent evaporation method. Briefly, 6 mL DCM containing defined amounts of PLA was added to the MMC–SPC complex (60 mg), followed by gentle agitation until a micelle solution was obtained. The solution was poured into defined amounts of aqueous solution containing 0.25% PVA and then probe sonicated at 80 W for 5 s and repeated three times in an ice-water bath to form a stable o/w emulsion. After evaporation of the organic solvent with gentle stirring under atmospheric pressure for 24 h, the complex and polymer gradually co-precipitated in the emulsion droplets, so MMC–PLA–SPC nanoparticles were obtained. Those solidified nanoparticles were collected by ultracentrifugation, washed with distilled water three times, and lyophilized.

The drug entrapment efficiency (EE%) was determined indirectly by measuring the amount of free MMC using UV/vis spectrometer at 365 nm in the supernatant recovered after ultracentrifugation. The drug entrapment

efficiency was expressed as percentage of the MMC difference between the initial amount of MMC and the free amount in the supernatant relative to the total amount used for the nanoparticles preparation.

To compare the results and those obtained by a classical method, the PLA–MMC microparticles were also prepared by a double emulation solvent evaporation method. The procedure for PLA–MMC microparticles was similar to the process mentioned above except that 6 mL DCM containing defined amounts of PLA was added to 3 mL of distilled water solution containing 10 mg MMC, and probe sonicated at 80 W for 5 s and repeated three times in an ice-water bath to form a w_1/o primary emulsion, and followed by the w_1/o emulsion droplets were poured into defined amounts of aqueous solution containing 0.25% PVA and homogenized at a rate of 1000 rpm.

Formulation Optimization

An orthogonal $L_9(3^4)$ test design was used to investigate the optimal formulation condition. As seen from Table 1, the optimal experiment was carried out with four factors and three levels, namely PLA MW, ratio of PLA to SPC (w/w), the ratio of MMC to SPC (w/w), volume ratio of oil phase to water phase (labeled as A, B, C, and D in Table 1). The range of each factor level was based on the results of preliminary experiments using a single-factor test. The entrapment efficiency (EE%) of MMC was the dependent variable. The PLA–MMC–SPC nanoparticles obtained from the above nine tests were operated following the method mentioned above. The $L_9(3^4)$ orthogonal design was established as shown in Table 1.

Characterization of PLA–MMC–SPC Nanoparticles

SEM (XL-30, Philips) was used to examine the surface morphology of PLA–MMC–SPC nanoparticles. The dried nanoparticles were mounted on metal stubs with double-sided electrical tape. They were gold coated under reduced pressure with a sputter coater before being viewed under the SEM at 20 kV. Zetasizer (Nano-ZS, Malven) was used to measure the size distribution and Zata potential of PLA–MMC nanoparticles. Prior to analysis, 10 mL of distilled water was added to a 20 mL vial containing PLA–MMC–SPC nanoparticles powder (containing 10 mg), and the vial was shaken. The characterization of PLA–MMC microparticles prepared by classical method was also examined in the same way as used for comparison.

Table 1 Factor-level in orthogonal-design experiments of L_9 (3^4)

Level	Factor			
	A PLA MW	B PLA/SPC	C MMC/SPC	D O/W
1	5000	1:1	1:10	1:2.5
2	10000	3:1	2:10	1:5
3	50000	5:1	3:10	1:10

A The molecular weight of PLA, *B* the ratio of PLA to SPC (wt/wt), *C* the ratio of MMC to SPC (wt/wt), *D* the ratio of oil to water solution (v/v)

Assay of In Vitro Drug Release

The in vitro release of MMC from the PLA–MMC–SPC nanoparticles was measured in PBS at pH 7.2. PLA–MMC–SPC nanoparticles weighing 40 mg were added in 50 mL of the medium in 60 mL conical screw capped tubes, preserved with 0.05% (w/v) sodium azide to prevent microbial growth. The samples were incubated at 37 °C and shaken horizontally at 100 cpm in a shaking incubator. At given time intervals, samples were removed from the vials tubes for quantitative estimation of the amount of drug released. In a typical test, 0.5 mL of the drug containing buffer solution was removed and the vial was replenished with 0.5 mL of fresh buffer solution to maintain a constant volume of the released medium. All release tests were run in triplicates.

The release of MMC from PLA–MMC microparticles was also measured in the same way as used for comparison.

Results and Discussion

The pictures of SPC, MMC, their physical mixture, and complex in organic solvent (DCM) before and after 24 h storage are shown in Figs. 1 and 2. It is clear to see that MMC–SPC complex is dissolved in the DCM completely (Fig. 1d) and stable even after 24 h storage (Fig. 2d).

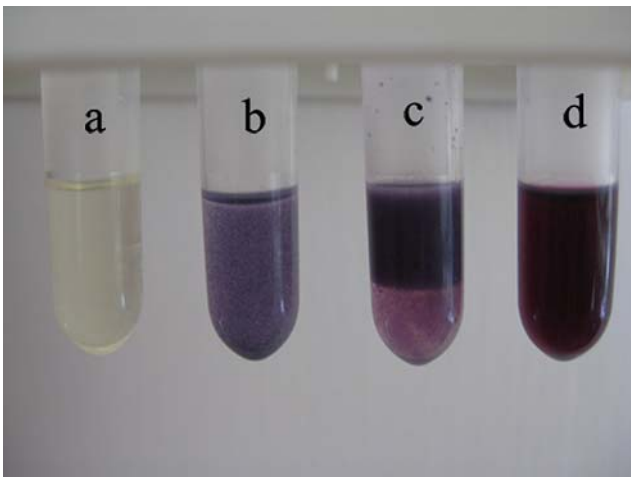

Fig. 1 The pictures of SPC (**a**), MMC (**b**), their physical mixture (**c**), and complex (**d**) in organic solvent (DCM) before storage

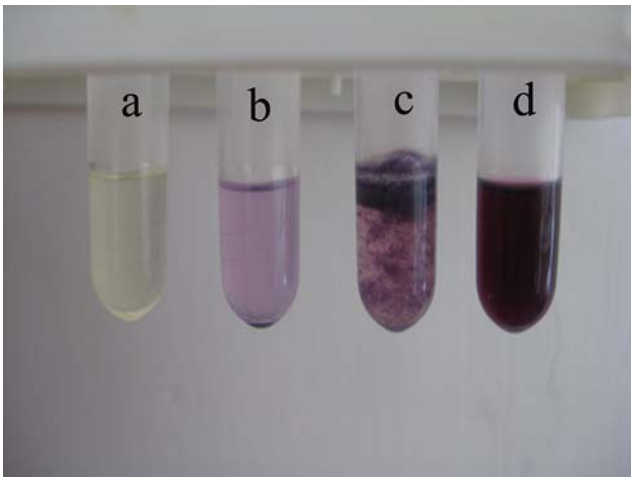

Fig. 2 The pictures of SPC (**a**), MMC (**b**), their physical mixture (**c**), and complex (**d**) in organic solvent (DCM) after 24 h storage

However, a separation layer is shown for the corresponding physical mixture (Fig. 1c and Fig. 2c), which suggests that MMC could not be solubilized effectively within DCM by simple physical mixing with SPC. As MMC cannot be soluble in DCM (Fig. 1b) it precipitates after 24 h of storage (Fig. 2b). The results could be explained by that the hydrophilic head group of SPC may be directed toward the hydrophilic areas of MMC and the hydrophobic tail is directed toward the organic phase to provide the correct orientation. This explanation is further confirmed by FTIR experiments, which will be discussed below.

FTIR analysis is used to study the interactions between MMC and SPC. The infrared spectra of MMC and SPC, their physical mixture and complex are shown in Fig. 3. There was a significant difference between the physical mixture (Fig. 3d) and the complex (Fig. 3c). The spectrum of the physical mixture shows an additive effect of MMC and SPC, in which the characteristic absorption peaks of MMC (Fig. 3a) at 3345 cm^{-1}, 3316 cm^{-1}, 3269 cm^{-1} are present in one broad absorption peak. However, in the spectrum of their complex, the three characteristic absorption peaks of MMC are almost masked by that of SPC. Compared with SPC (Fig. 3b), the characteristic absorption peak at 1231 cm^{-1} of SPC disappears in the spectrum of the complex. Moreover, no new peaks are observed in the mixture and complex. These observations suggest that some weak physical interactions between MMC and SPC take place during the formation of the complex.

The analysis results of orthogonal test performed by statistical software SPSS 13.0 are presented in Table 2. The factors influencing the EE (%) are listed in a decreasing order as follow: B > C > D > A according to the *R* value and the individual levels within each factor are ranked as: A: 1 > 3 > 2; B: 2 > 3 > 1; C: 2 > 1 > 3; D: 1 > 2 > 3. The optimized formulation should be $B_2C_2D_1A_1$ (the ratio of PLA to SPC: 3:1, the ratio of MMC to SPC: 2:10, the ratio of oil to water solution: 1:2.5, and PLA MW: 5000), according to the *R* value, we can find the ratio of PLA to SPC is found to be the most important determinant of the EE (%). However, the factor of PLA MW can be overlooked. Through confirmatory test, the drug entrapment efficiency is up to as high as 94.8%, while that prepared by classical method at same condition is

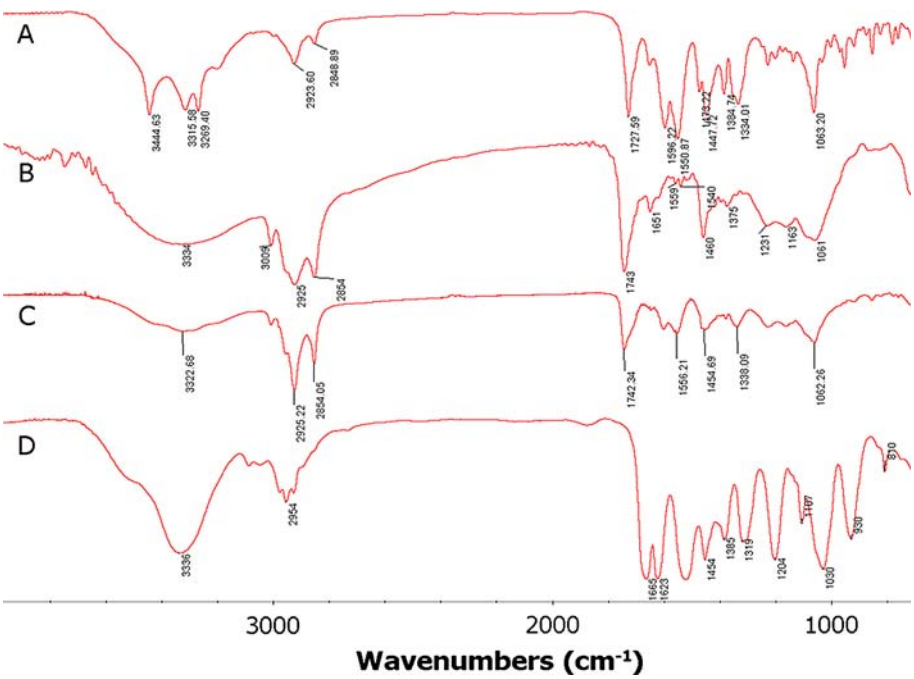

Fig. 3 The FTIR of MMC (a) and SPC (b), complex (c), and their physical mixture (d)

Table 2 Result of orthogonal-design experiments L_9 (3^4)

No.	A	B	C	D	EE (S1)
1	1	1	1	1	70.53
2	1	2	2	2	88.75
3	1	3	3	3	80.45
4	2	1	2	3	65.98
5	2	2	3	1	83.67
6	2	3	1	2	87.20
7	3	1	3	2	60.46
8	3	2	1	3	86.45
9	3	3	2	1	90.36
S1 K1	79.91	65.66	81.39	81.52	
K2	78.95	86.29	81.70	78.80	
K3	79.09	86.00	74.86	77.63	
R	0.96	20.63	6.84	3.89	

A The molecular weight of PLA, *B* the ratio of PLA to SPC (wt/wt), *C* the ratio of MMC to SPC (wt/wt), *D* the ratio of oil to water solution (v/v), *EE*(%) drug entrapment efficiency

34.5%. Those significant differences may be due to the reason that high liposolubility of MMC–SPC and affinity of MMC and SPC make MMC being trapped in the nanoparticles with little MMC released into the external water phase or destroyed during the preparation.

The SEM image of both PLA–MMC–SPC nanoparticles (a, c) and PLA–MMC microparticle (b, d) are shown in Fig. 4, which demonstrates that both nanoparticles and microparticles are essentially spherical in shape, but there are many pinholes in the surface of microparticles. The cross-sectional SEM image of both PLA nanoparticles (c) and microparticles (d) could be seen by breaking them, showing inner empty structure, but shell of PLA nanoparticles is relatively thicker than that of microparticles. There exist two possibility of the position of encapsulated drugs after removing the dichloromethane in the preparation of PLA nanoparticles, one possibility is that the encapsulated drugs are uniformly dispersed with the PLA nanoparticles, another possibility is that the encapsulated drugs are loaded into the inner part of PLA particles, forming a shell core structure (same like the egg) or layer structure, but this shell core or layer structure was not found from the cross-sectional SEM image of PLA nanoparticles, indicting that drug is uniformly dispersed within the shell of PLA nanoparticles.

The zeta potential value (−42.2 mV) observed for PLA–MMC–SPC nanoparticles is significantly lower than −30 mV, the typical threshold value for flocculation [12], suggesting the suspension shows well stability, while zeta potential value for the PLA–MMC microparticles is found to be −12.6 mV. This significant difference of zeta potential value between PLA–MMC–SPC nanoparticles and PLA–MMC microparticles can be explained by the fact that SPC is an amphiphile and can be served as a surfactant; there was a minimal free SPC on their surface with hydrophilic head group of SPC toward the suspending medium during the formation of PLA–MMC–SPC nanoparticles.

A particle size distribution of PLA–MMC–SPC nanoparticles is shown in Fig. 5. Result shows that an average diameter of PLA–MMC–SPC nanoparticles is 594 nm with a narrow size distribution, while those prepared by the classical method present very broad size distribution

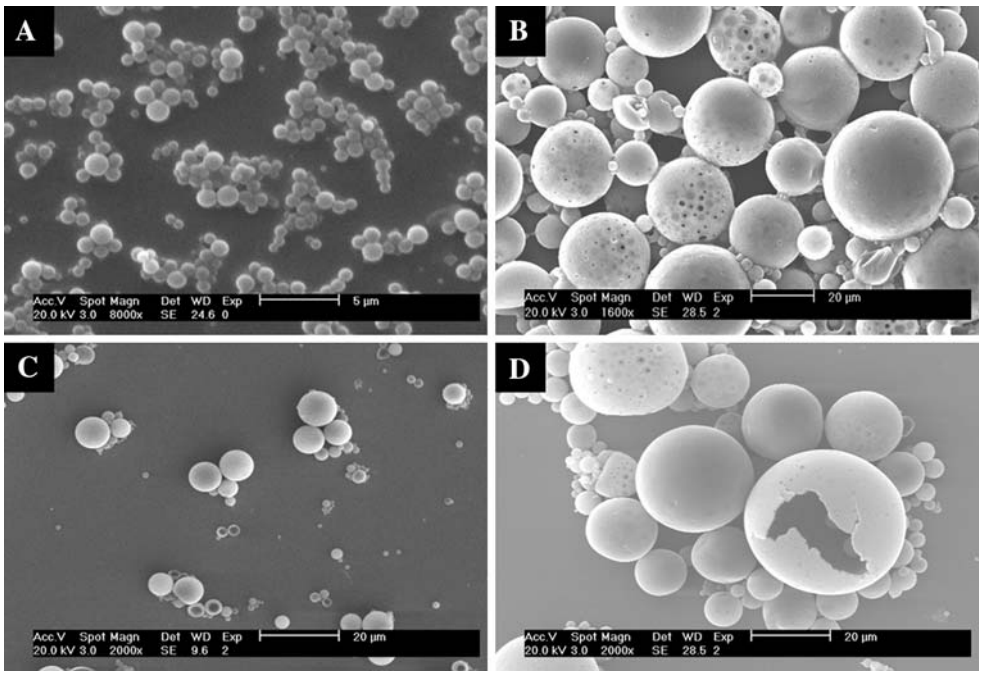

Fig. 4 SME image of PLA–MMC–SPC nanoparticles prepared by new single solvent evaporation method (**a**, **c**) and PLA–MMC microparticles prepared by the classical method (**b**, **d**)

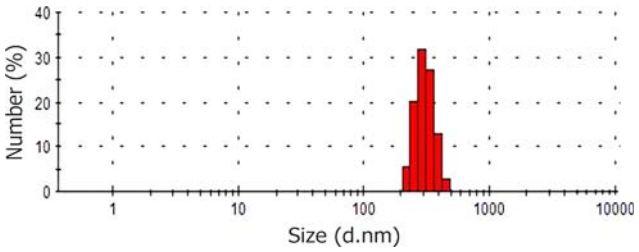

Fig. 5 Size distribution of PLA-MMC-SPC nanoparticles prepared by a new single solvent evaporation method

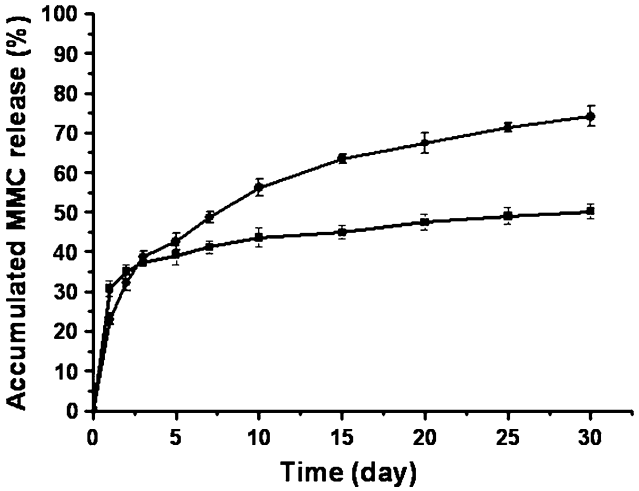

Fig. 6 Release of MMC from particles prepared with different methods. Prepared by a new single solvent evaporation method (*black square*), prepared by a classical method (*black circle*)

and the average diameters of 6.44 μm (figure was not presented).

The in vitro release profiles of MMC from the PLA–MMC–SPC nanoparticles and the PLA–MMC microparticles are monitored as a function of time (Fig. 6). As seen in Fig. 6, the amount of MMC released from the PLA–MMC–SPC nanoparticles at pH 7.2 medium is 30.76% over 24 h, whereas that of free MMC released from the PLA–MMC microparticles is no more than 23.00%. This difference is probably due to the fact that smaller sized PLA–MMC–SPC nanoparticles are subject to a more extensive MMC release by diffusion toward the suspending medium due to their higher surface volume ratio. This phenomenon also suggests that the MMC–SPC complex trapped on the surface of the nanoparticles has suffered dissociation and MMC could be released as free form. Following the initial rapid release phase, both of them have a sustained drug release phase and a cumulated drug release over 30 days is 50.17% for PLA–MMC–SPC nanoparticles and 74.10% for PLA–MMC microparticles. This difference may be explained by the interaction between the negatively charged phosphate group in SPC and positively charged amino group in MMC, which guarantees the integrity of MMC–SPC complex being released from the nanoparticles first and then followed by the MMC dissociation from the complex in the pH 7.2 PBS medium. In addition, integrity of MMC–SPC complex also prevents the labile amino group of MMC from being broken down at low pH surrounding. Actually, the real reason requires further studies.

Conclusion

This work demonstrates that the new single emulsion solvent evaporation method for the encapsulation of MMC in PLA nanoparticles results in improved formulation characteristics including smaller size, lower size distribution, higher encapsulation yield, and longer sustained drug release in comparison to classical method. The PLA–MMC–SPC nanoparticles system has a potential for long sustained delivery of MMC for local administration especially at tumor tissues and efficacy studies with these systems are underway.

Acknowledgments This work was supported by the National Basic Research Program of China (2006CB933300) and the National Key Technology R&D Program (2007BAD07B05).

References

1. A.M. Rauth, J.K. Mohindra, I.F. Tannock, Cancer Res. **43**, 4154 (1983)
2. S. Rockwell, C.S. Hughes, Cell Prolif. **27**, 153 (1994). doi:10.1111/j.1365-2184.1994.tb01413.x
3. J. Cummings, L. Allan, J.F. Smyth, Biochem. Pharmacol. **47**, 1345 (1994). doi:10.1016/0006-2952(94)90333-6
4. T. Nomura, A. Saikawa, S. Morita, T. Sakaeda, F. Yamashita, K. Honda, J. Control. Release **52**, 239 (1998). doi:10.1016/S0168-3659(97)00185-5
5. Y.C. Richard, Y. Yuming, M.R. Andrew, M. Norman, Biomaterials **26**, 5375 (2005). doi:10.1016/j.biomaterials.2005.01.050
6. N. Ishiki, H. Onishi, Y. Machida, Int. J. Pharm. **279**, 81 (2004). doi:10.1016/j.ijpharm.2004.04.017
7. H. Onishi, H. Takahashi, M. Yoshiyasu, Y. Machida, Drug Dev. Ind. Pharm. **27**, 659 (2001). doi:10.1081/DDC-100107322
8. Y. Liu, H. Li, X.Z. Shu, S.D. Gray, G.D. Prestwich, Fertil. Steril. **83**, 1275 (2005). doi:10.1016/j.fertnstert.2004.09.038
9. X.X. Yang, J.H. Chen, S.T. Liu, D. Guo, X.X. Zeng, Regul. Toxicol. Pharmacol. **46**, 211 (2006). doi:10.1016/j.yrtph.2006.07.008
10. C. Sarısözen, Y. Aktaş, A. Mungan, E. Bilensoy, Eur. J. Pharm. Sci. **32**, S36 (2007). doi:10.1016/j.ejps.2007.05.076
11. S. Benita, J.P. Benoit, F. Puisieux, C. Thies, J. Pharm. Sci. **73**, 1721 (1984). doi:10.1002/jps.2600731215
12. P.A. Webb, *Analytical Methods in Fine Particle Technology* (Micromeritics Instrument Corporation, Norcross, GA, 1997), p. 279